JOURNAL OF SOLID STATE CHEMISTRY **126,** 55–64 (1996)
ARTICLE NO. 0310

Synthesis of $(BiPb)_2Sr_2Ca_2Cu_3O_y$ Superconductors by the Sol–Gel Process[1]

G. V. Rama Rao,* U. V. Varadaraju,† S. Venkadesan,* and S. L. Mannan*,[2]

*Materials Development Division, Indira Gandhi Centre for Atomic Research, Kalpakkam 603 102, India; and †Materials Science Research Centre, Indian Institute of Technology, Madras 600 036, India

Received January 3, 1996; in revised form May 7, 1996; accepted June 12, 1996

The sol–gel process is employed to synthesize single-phase lead-doped $Bi_2Sr_2Ca_2Cu_3O_{10}$ ((Bi,Pb)-2223) superconductors. The composition which can yield single-phase (Bi,Pb)-2223 compound is arrived at by varying the calcium and copper concentrations. Samples prepared with the composition $Bi_{1.68}Pb_{0.32}Sr_{1.75}Ca_{1.8}Cu_{2.8}O_y$ result in the formation of phase pure compound. The mechanism of formation of this compound and the intermediate steps involved during the phase formation are established by X-ray diffraction (XRD) and differential thermal analytical (DTA) studies. It is found that (Bi,Pb)-2223 phase formation occurs through the reaction of (Bi,Pb)-2212 phase with Ca_2CuO_3 and CuO in the liquid phase obtained from the partial melting calcium rich Bi-2212 phase. The stability region for the (Bi,Pb)-2223 compound is identified as 1118 to 1138 K. Several incongruent melting reactions are identified from XRD and DTA studies during the decomposition of Bi-2223 compound.

1. INTRODUCTION

Superconductivity in a Bi–Sr–Cu–O system at relatively low temperatures was first reported by Michel *et al.* (1). Addition of calcium to this system leads to the formation of two new superconducting phases with high and low transition temperatures (T_c = 110 and 80 K) (2). Although the nominal composition of the high T_c phase is proposed to be $Bi_2Sr_2Ca_2Cu_3O_y$ (2223), a single phase of this compound is difficult to prepare from the corresponding mixture of raw materials (3) and the high T_c phase is very sensitive to the composition of the starting mixture. It is found that 2223 single phase can be obtained with the addition of lead (4, 5). However, the low T_c phase $Bi_2Sr_2CaCu_2O_y$ (2212) is usually found to coexist with the 2223 phase even with the lead addition and the lead-doped phase is designated as (Bi,Pb)-2223. This led to several studies on the dependence of the fraction of high T_c phase on the starting composition (6, 7), reaction temperature (8), and annealing conditions (9). Sasakura *et al.* (10) have carried out extensive studies on the phase formation in the bismuth cuprate system and have constructed the partial phase diagram in air for the solid state reaction route. They have determined the compositional range over which single phase formation results.

The (Bi,Pb)-2223 phase synthesized by solid state route is always associated with 2212 phase, and even with prolonged annealing at high temperatures, it is difficult to eliminate the presence of 2212 phase. Moreover, prolonged annealing at high temperatures leads to loss of volatile elements such as Bi and Pb. Hence for the preparation of phase pure (Bi,Pb)-2223 compound other nonconventional synthetic methods are to be adopted. It is well known that the sol–gel method is superior to the conventional solid state reaction because in the former it is possible to mix the starting materials at the molecular level and the resulting product is expected to be homogeneous (11). There are several reports available in the literature on the synthesis of (Bi,Pb)-2223 compound by the sol–gel process (12–14). However, very few systematic studies are reported on compositional variation and on evolution of (Bi,Pb)-2223 phase using the sol–gel process (13). In this paper we report on the synthesis of (Bi,Pb)-2223 phase by the sol–gel process. We have chosen only the compositions in the single-phase region in the phase diagram reported by Sasakura *et al.* (10). The mechanism of formation of the (Bi,Pb)-2223 phase from the gels and its stability at high temperatures are discussed in detail.

2. EXPERIMENTAL

The compounds with the nominal compositions of the mixture taken as $Bi_{1.68}Pb_{0.32}Sr_{1.75}Ca_xCu_yO_z$, where $1.75 \leq x \leq 1.85$ and $2.65 \leq y \leq 2.85$, are synthesized. Bismuth nitrate is dissolved in acetic acid. Appropriate amounts of strontium nitrate, acetates of calcium, and copper are dissolved in ammonia water and then added to bismuth nitrate solution. Lead acetate is dissolved in water and

[1] This work forms part of the Ph.D. thesis of G.V.R.R.
[2] To whom correspondence is to be addressed.

0022-4596/96 $18.00

added to the above solution. The pH of the solution is adjusted to 5.5 by addition of ammonia solution. The solution thus obtained is stirred for 5 h at room temperature, kept in an oven at 343 K to increase the viscosity of the solution, and set into a transparent gel by cooling to room temperature. Gels are characterized by infrared spectroscopy (Digilab, FTIR), thermogravimetry, differential thermal analysis (Polymer STA 1500 & Setaram), and scanning electron microscopy (Phillips PSEM502). Thermoanalytical characterizations (TG and DTA) are carried out in air using 8–10 mg of the sample at a heating rate of 10°/minute. Gels are decomposed at 723 K/5 h and calcined at 1068 K/15 h. The powder thus obtained is ground and pelletized and heat treated at 1123 K for 90 h. The pellets are reground and again compacted and heat treated at 1123 K/60 h, followed by slow cooling to 973 K and by furnace cooling to room temperature. Powders obtained after every heat treatment are characterized by X-ray diffraction (XRD) using Cu$K\alpha$ using a computer-controlled Seifert (P 3000) diffractometer. Particle sizes of the powders are determined by using Malvern Zeta Sizer-3 and Malvern E 3600 particle size analyzer. Surface areas of the powders are also determined by standard BET techniques using a Quantasorb Jr. surface area analyzer. Sintered pellets are polished and the morphology is observed in SEM. The compositional homogeneity is established by EDAX analysis. Superconductivity properties are evaluated by van der Pauw four-probe resistivity and a.c. susceptibility measurements on sintered pellets. The chemical composition of the superconducting phase is estimated using atomic absorption and emission spectroscopy.

To study the evolution of the (Bi,Pb)-2223 phase from the gels, the gel samples are heat treated at different temperatures for 1 h and are air quenched from heat treatment temperatures and then characterized by XRD. DTA experiments are carried out on phase pure (Bi,Pb)-2223 compound in both heating and cooling cycles to study its decomposition on heating and its crystallization of the phases during cooling.

3. RESULTS AND DISCUSSION

3.1. Standardization of the Composition for the Single-Phase Formation of (Bi,Pb)-2223 Compound

Table 1 shows the phases formed at various temperatures of the samples prepared with different compositions. Samples heat treated at 1068 K/15 h consist of both 2201 and 2212 phases, while 1123 K/90 h heat-treated sample contain a mixture of 2212 and (Bi,Pb)-2223 phases. On further heat treatment at 1123 K/65 h only a few compositions yield phase pure (Bi,Pb)-2223 compound. Figure 1 shows the XRD patterns of samples heat treated at 1123 K/90 h followed by 1123 K/65 h for various compositions. Only samples prepared with compositions of $Bi_{1.68}Pb_{0.32}Sr_{1.75}$

TABLE 1
Formation of Various Phases with Variation in Calcium and Copper Contents ($Bi_{1.68}Pb_{0.32}Sr_{1.75}Ca_xCu_yO_z$) in the Samples Heat Treated at 1123 K for 90 + 60 h

	Copper (y)				
Calcium (x)	2.65	2.7	2.75	2.8	2.85
1.77	2212	2212, 2223	2212	2223	2212, 2223, Ca_2PbO_4
1.8	2212 Ca_2PbO_4	2212, 2223, Ca_2CuO_3	2212, 2223, Ca_2PbO_4	2223	2212, 2223
1.83	2212, 2223	2212	2212, 2223, Ca_2PbO_4, Ca_2CuO_3	2223	2212

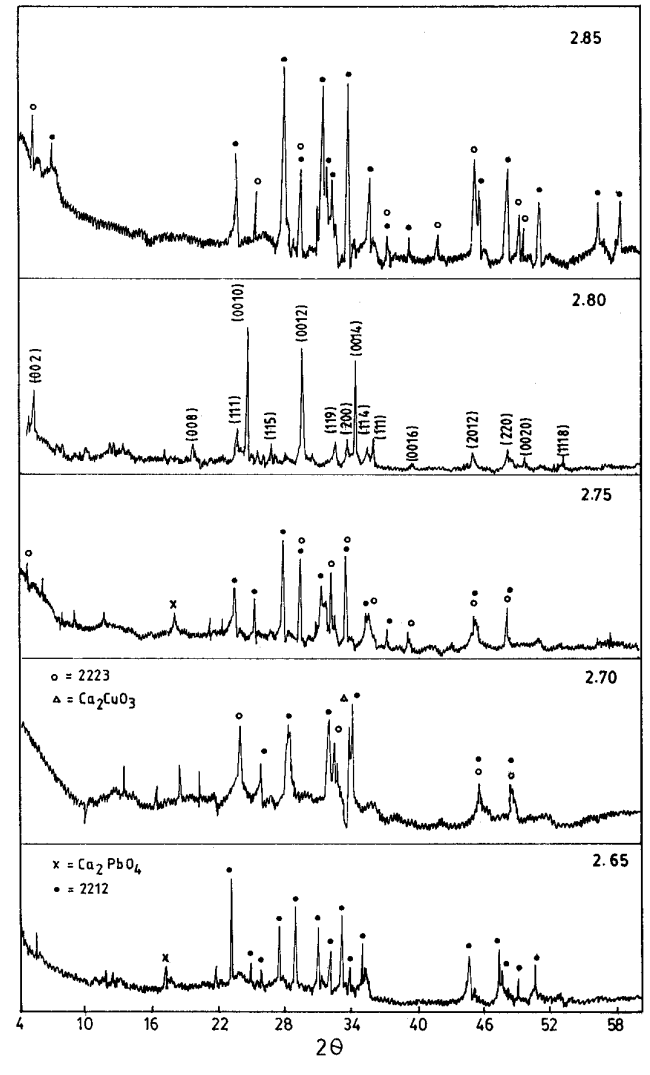

FIG. 1. XRD patterns of the samples heat treated at 1123 K/90 h and 1123 K/60 h for various compositions.

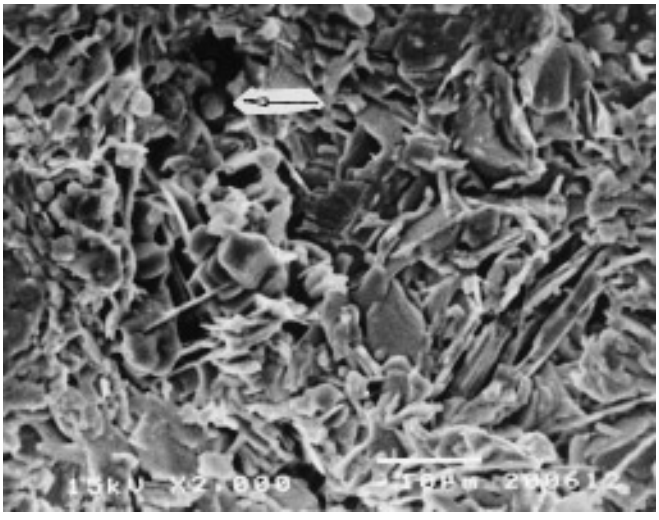

FIG. 2. SEM picture of sintered pellets of $Bi_{1.6}Pb_{0.32}Sr_{1.75}Ca_{1.8}Cu_{2.8}O_y$.

$Ca_{1.8}Cu_{2.8}O_z$ and $Bi_{1.68}Pb_{0.32}Sr_{1.75}Ca_{1.8}Cu_{2.8}O_y$ show the formation of single-phase (Bi,Pb)-2223 compound, whereas other compositions result in formation of both 2212 and (Bi,Pb)-2223 phases. The lattice parameters are evaluated for the above two compositions and are found to be a = 5.413 Å and c = 37.115 Å. These values are in excellent agreement with the values reported in the literature (15). Even though XRD patterns do not indicate the impurity phase formation, secondary phases are observed in SEM pictures (Fig. 2) and are identified as calcium plumbate from EDAX measurements. EDAX analysis reveals good compositional homogeneity from grain to grain, whereas it is very difficult to achieve compositional homogeneity in the samples prepared from the solid state route. Chemical compositions of the bulk obtained from AAS measurements match well with the starting compositions and no lead loss is observed. The highly reactive precursor powders (particle size 0.1–0.4 μm and specific surface area 65 m^2/g) obtained on gel decomposition are responsible for formation of (Bi,Pb)-2223 phase in a shorter annealing time of 150 h. The particle size of the (Bi,Pb)-2223 powders is found to be in the range 1–3 μm and with specific surface area of 8 m^2/g.

Resistivity measurements show superconducting onset at 115 K with $T_{c,zero}$ at 105 K (Fig. 3). Susceptibility measurements show a sharp diamagnetic transition at 106.5 K and a second drop at 94 K (Fig. 4). The second drop cannot be due to an impurity second phase since the T_c values of

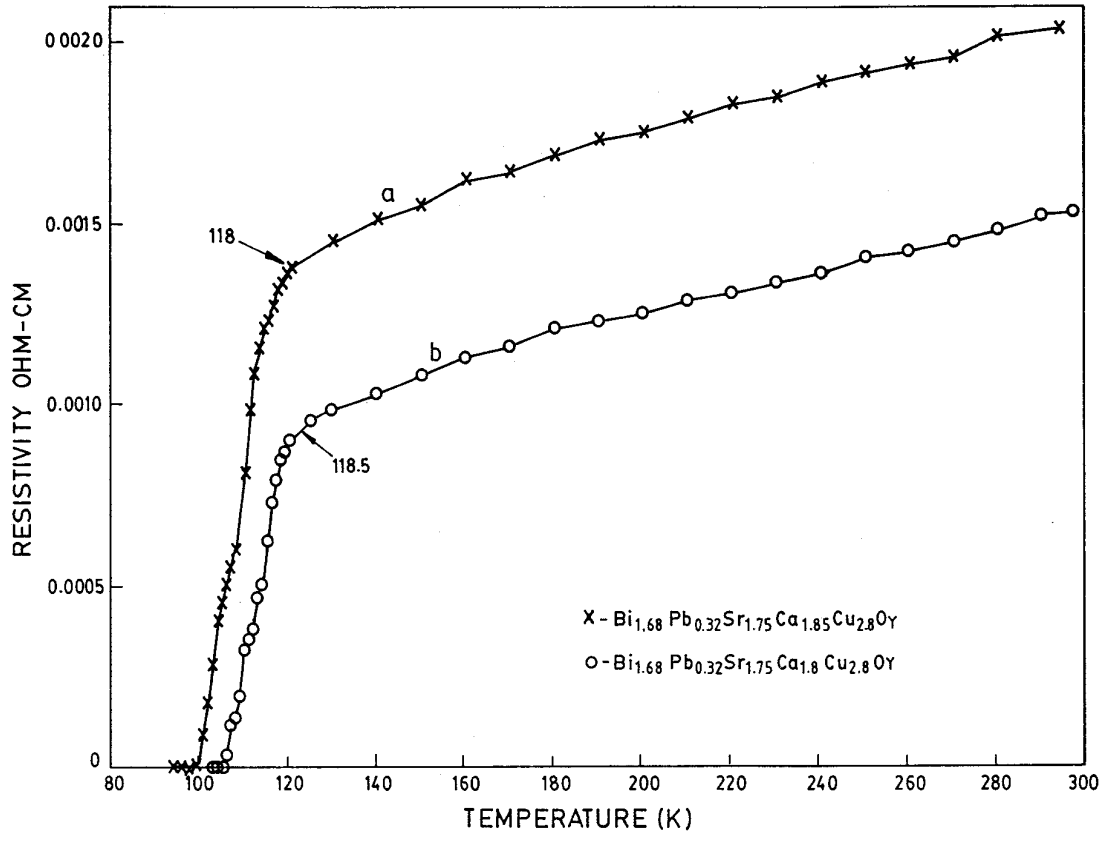

FIG. 3. ρ–T plots for (Bi,Pb)-2223 samples.

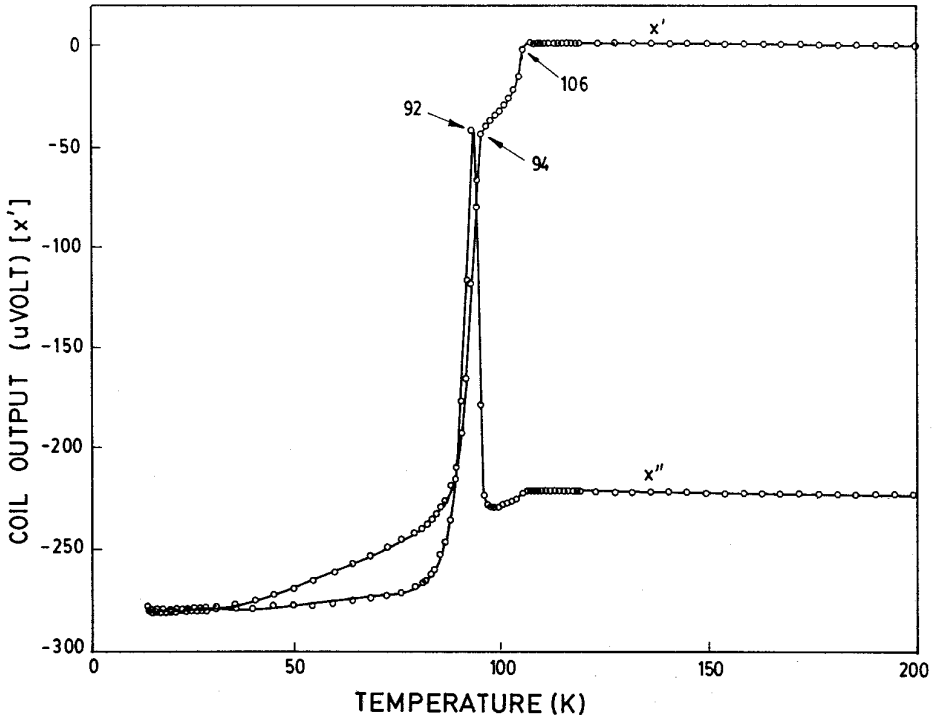

FIG. 4. χ–T plots for (Bi,Pb)-2223 samples.

the two possible superconducting phases in the bismuth system corresponding to 2201,2212 have highest T_c's of 20 and 85 K, respectively. Also the XRD shows single-phase (Bi,Pb)-2223, and any impurity which is within the limits of the detection (5%) cannot give rise to such a strong diamagnetic signal. It is well known that the bismuth cuprate system exhibits distinct granular behavior (16). Hence, the two drops corresponding to diamagnetic signal

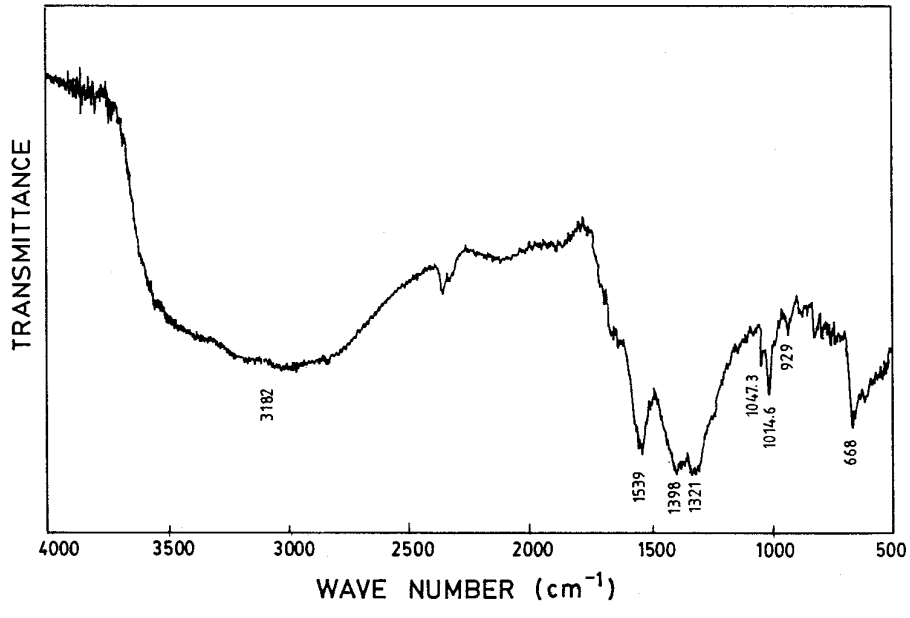

FIG. 5. IR spectra of the precursor gel.

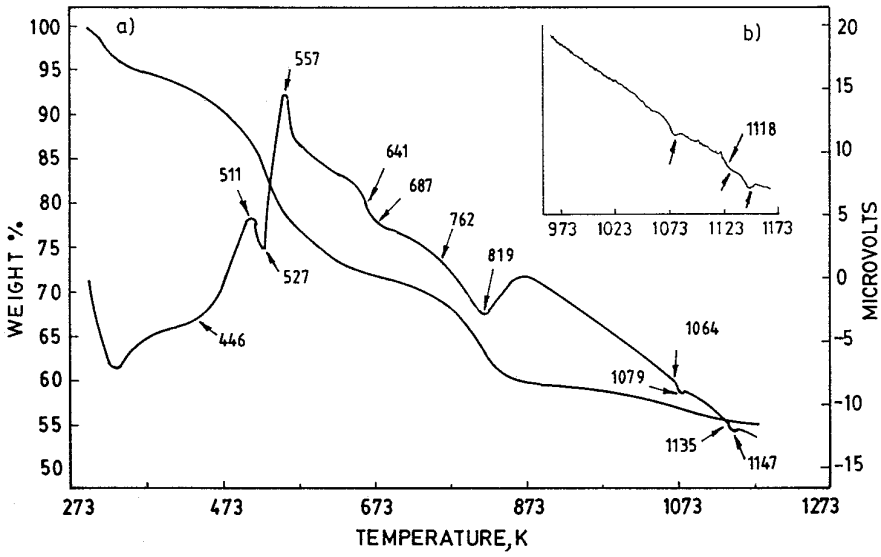

FIG. 6. (a) TG and DTA patterns of the gel samples. (b) shows the expanded region of the DTA pattern.

are due to superconductivity of the grains (T_c grain) and the bulk (T_c, bulk) of the sample, respectively. The χ''–T plot shows a single sharp peak at 92 K, confirming the homogeneity of the sample (Fig. 4).

3.2. Gel Characterization

To understand the bonding of the metal ions in the gels and the mechanism of formation of the (Bi,Pb)-2223 compound, further investigations are carried out on the gel samples of single-phase compositions (viz., $Bi_{1.68}Pb_{0.32}Sr_{1.75}Ca_{1.8}Cu_{2.8}O_{10}$) by IR, TG, DTA, and XRD techniques. Figure 5 shows the IR spectra of the gel. The band at 3188 cm^{-1} indicates the ν_{O-H} of the hydrogen-bonded water molecules. The two strong bands at 1536 and 1398 cm^{-1} correspond to asymmetric and symmetric stretching frequencies of the COO group. The separation between the asymmetric and symmetric stretching frequencies ($\Delta\nu$) of the COO group indicates the bonding of carboxylate groups to the metal ions. The $\Delta\nu$ obtained from the IR spectra of the gel is 141 cm^{-1}. According to Deacon and Phillips (17), the $\Delta\nu$ in the range of 110–160 cm^{-1} indicates that the carboxylate group is participating in the bridging type of bonding with the metal ions. In general, gelation occurs through the polymerization and condensation of metal hydroxides resulting in M–O–M linkage. There are no bands below 600 cm^{-1}. This indicates the absence of M–O–M bonds in the gel (18). Hence, the gelation in this system might have occurred through bridging of carboxylates groups to the metal ions followed by the polymerization of bridging carboxylate moieties. Similar behavior is reported in the synthesis of $YBa_2Cu_3O_7$ compounds by various gel routes (19, 20).

Figure 6 shows both TG and DTA patterns of the gel samples from RT to 1138 K. The weight loss is divided into four regions, 463–512, 512–660, 740–861, and 950–1123 K, and the total weight loss is found to be 46%. The weight loss in the first two temperature ranges is due to the decomposition of metal acetates and other organic groups present in the gel. The onset of both endo and exothermic peaks in DTA are shown in Fig. 6. The sharp endotherm at 503 K corresponds to loss of water from the gel followed by a sharp exotherm at 526 K corresponding to decomposition of acetates. The endotherms at 640 and 762 K are due to the formation of carbonates and formation of Bi-2201, respectively.

3.3. Mechanism of Formation of (Bi,Pb)-2223 Compound

The weight loss in the two temperature regions 740–861 and 950–1123 K is due to the formation of different phases from their respective carbonates. This is further supported by the XRD patterns of the samples quenched from various

TABLE 2
Formation of Various Phases on Heat Treatment of Gel at Various Temperatures

Sample no.	Temperature (K)	Phases observed
1	673	Bi_2O_3, $SrCO_3$, $CaCO_3$, CuO, PbO
2	873	2201, $CaCO_3$, CuO, PbO
3	973	2201, $(Ca_{1-x}Sr_x)CO_3$, CuO, PbO, $CaCO_3$
4	1023	2201, Ca_2PbO_4, CuO, $CaCO_3$, $(Ca_{1-x}Sr_x)CO_3$
5	1073	2212, $CaCO_3$, Ca_2PbO_4, CuO
6	1123	2223, 2212, $CaCO_3$, CuO

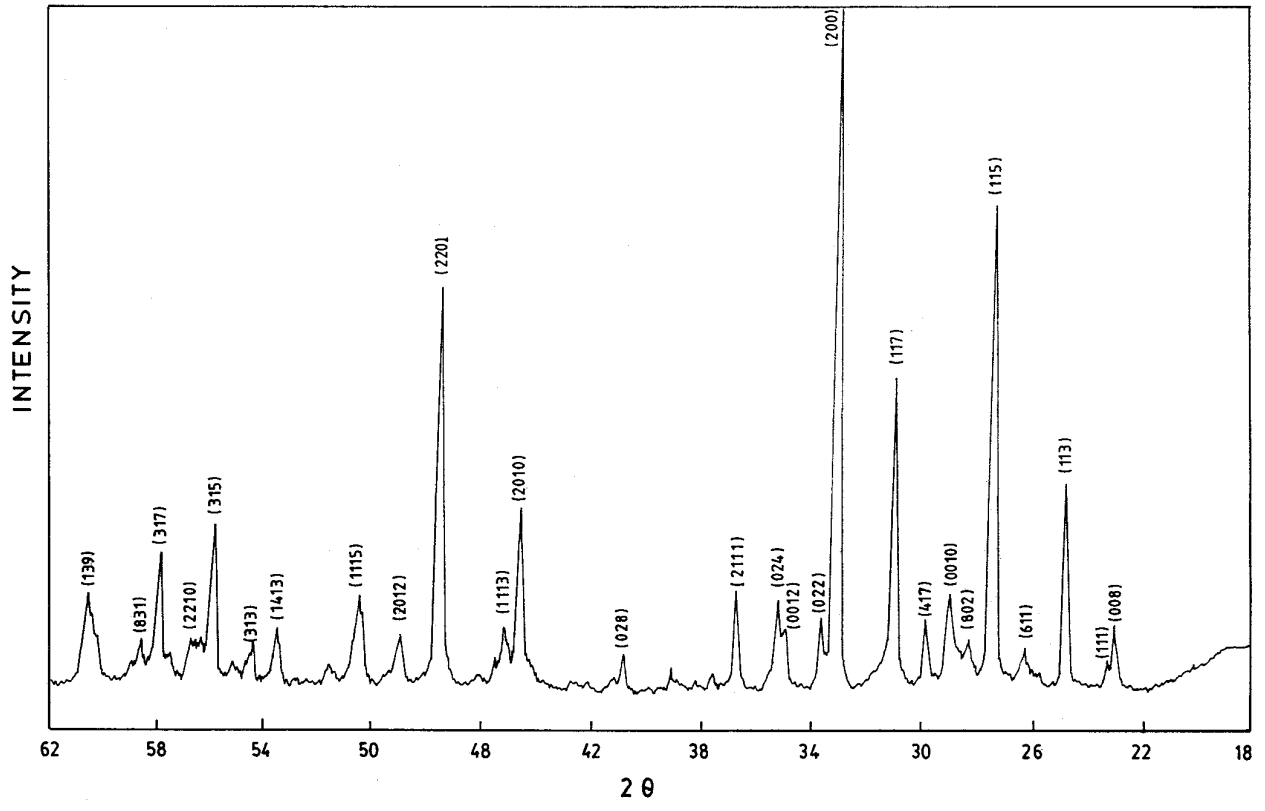

FIG. 7. XRD patterns of sample heat treated at 1103 K/600 h.

temperatures (Table 2). The XRD of the gel is amorphous and the phases formed at different temperatures are shown in Table 2. An endotherm at 762 K and the weight loss in the temperature region 740–861 is due to the formation of Bi-2201 phase. The samples quenched from 873 K show the formation of 2201 whereas the samples quenched from 973 K contain strontium-deficient 2201 phase along with (Sr, Ca)CO_3 phase. It is reported in the literature that at higher temperatures, a more stable strontium deficient 2201 phase forms through the disproportionation of stoichiometric 2201 phase (21). A systematic study is carried out in the literature to find out the stability of the compound $Bi_2Sr_xCuO_y$, where $1.3 \leq x \leq 2.1$ (21), and phases with $x = 1.7$ are found to be more stable.

The weight loss in the temperature region of 950–1123 K is due to the formation of various phases. The formation of calcium plumbate phase is observed in the samples quenched from 1023 K. An endotherm at 1063 K is due to the formation of 2212 phase, which is confirmed by the XRD pattern samples quenched from 1073 K. The onset temperatures of the last two endothermic peaks are at 1112 and 1135 K. It is reported in the literature that an endotherm at 1113 K is due to the melting of Bi_2CuO_4 phase (22) but this phase is not observed in the XRD patterns of the samples quenched from various temperatures (Table 2). Hence, the endotherm at 1113 K can not be attributed to the melting of Bi_2CuO_4 phase but may be related to the formation of (Bi,Pb)-2223 phase and/or to the melting of any other phase present in the sample. The other endotherm at 1135 K is due to the melting of (Bi,Pb)-2223 compound which matches well with the literature value (23). From these results the probable reaction sequences for the formation of (Bi,Pb)-2223 are as follows:

1. At 673 K

$$\text{Gel} \rightarrow Bi_2O_3 + SrCO_3 + CaCO_3 + CuO + PbO \quad [1]$$

2. 673–873 K

$$Bi_2O_3 + 2SrCO_3 + CuO \rightarrow Bi_2Sr_2CuO_6 + 2CO_2 \quad [2]$$

3. 873–973 K

$$Bi_2Sr_2CuO_6 + CaCO_3 \rightarrow Bi_2Sr_{2-x}CuO_6(2201) + (Ca_{1-x}Sr_x)CO_3 \quad [3]$$

4. 973–1023 K

$$2CaCO_3 + PbO \rightarrow Ca_2PbO_4 + CO_2 + 1/2O_2 \quad [4]$$

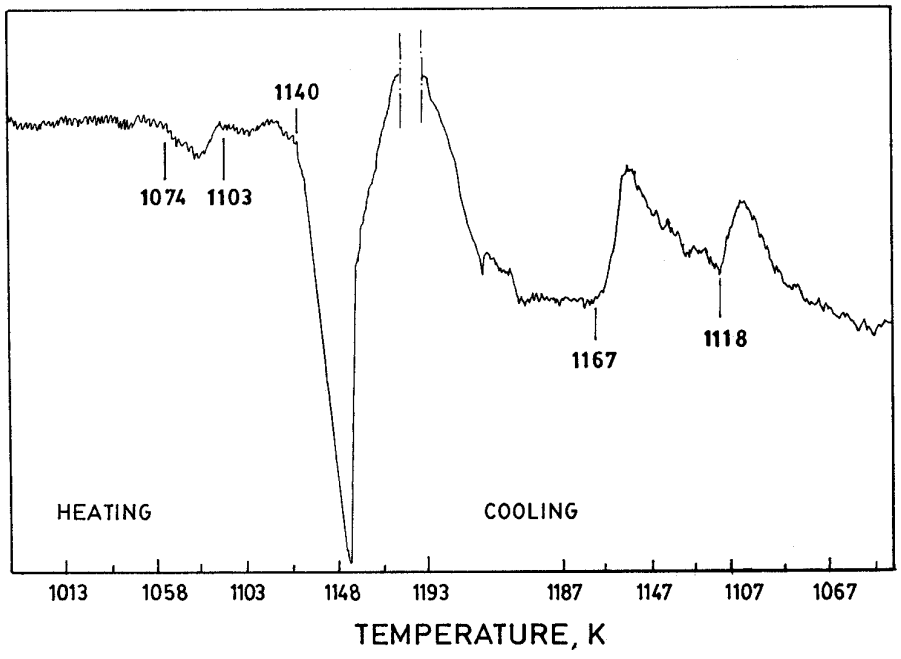

FIG. 8. DTA patterns of (Bi,Pb)-2223 sample showing the melting of the phase.

5. 1023–1073 K

$$2201 + CaCO_3 + (Ca_{1-x}Sr_x)CO_3 + CuO \rightarrow Bi_2Sr_2Ca_{1+x}Cu_2O_8(2212) + CO_2 \quad [5]$$

6. 1073–1123 K

$$2212 + CaCO_3 + CuO \rightarrow Bi_2Sr_2Ca_2Cu_3O_{10}(2223) + CO_2. \quad [6]$$

Although the XRD of the sample quenched at 1123 K showed the presence of (Bi,Pb)-2223 phase, the phase pure compound is obtained only after annealing for 150 h. During annealing calcium carbonate reacts with copper oxide to form Ca_2CuO_3 phase.

$$2CaCO_3 + CuO \rightarrow Ca_2CuO_3 + 2CO_2 \quad [7]$$

In fact, without lead doping the single-phase formation of Bi-2223 compound does not take place even with few weeks of annealing time. Due to the presence of lead the formation is taking place within a few days, so it is essential to understand the mechanism of reaction [6] and role of lead.

Search of literature shows that formation of (Bi,Pb)-2223 occurs during the melting of 2212 phase. It is also reported that (Bi,Pb)-2223 phase formation is more favorable when the melting point of the 2212 is lower than that of (Bi,Pb)-2223 (24, 25). Melting temperatures of the phases depend on their compositions. Without lead doping Bi-2212 compound has the melting point of 1163 K, while on lead doping the melting temperature comes down to 1145 K (24). Several methods for obtaining low melting 2212 phase, such as processing in reduced oxygen (26) and forming Ca-rich 2212 phase (27), are reported in the literature. Recently Dorris *et al.* (28) obtained the DTA patterns for all the calcium-rich phases and they found that the melting of one of the 2212 phase occurs at 1110 K, which coincides with the endotherm observed in the present study (1113 K). Although 2223 phase formation is observed in the samples heat-treated at 1113 K, the complete conversion to 2223 phase occurs only at 1123 K/150 h. This is due to the slow kinetics for the formation of (Bi,Pb)-2223 phase at 1113 K. The (Bi,Pb)-2223 phase formation can be written as

$$2212 + 1/2Ca_2CuO_3 + 1/2CuO \xrightarrow{\text{in partial melt of 2212}} Bi_2Sr_2Ca_2Cu_3O_{10}(2223) \quad [6a]$$

There are some reports that 2223 phase formation also occurs in the presence of eutectic liquid (29). Ikeda *et al.* (29) have carried out DTA for different samples with nominal combinations of 2201, Ca_2PbO_4, 2212, and CuO and showed that only a mixture of $2201 : Ca_2PbO_4 = 7:3$ with CuO gives a sharp endotherm at 1098 K. The presence of this liquid phase enhances the formation of 2223 phase at low temperatures (30). Hence reaction [6] can be rewritten as

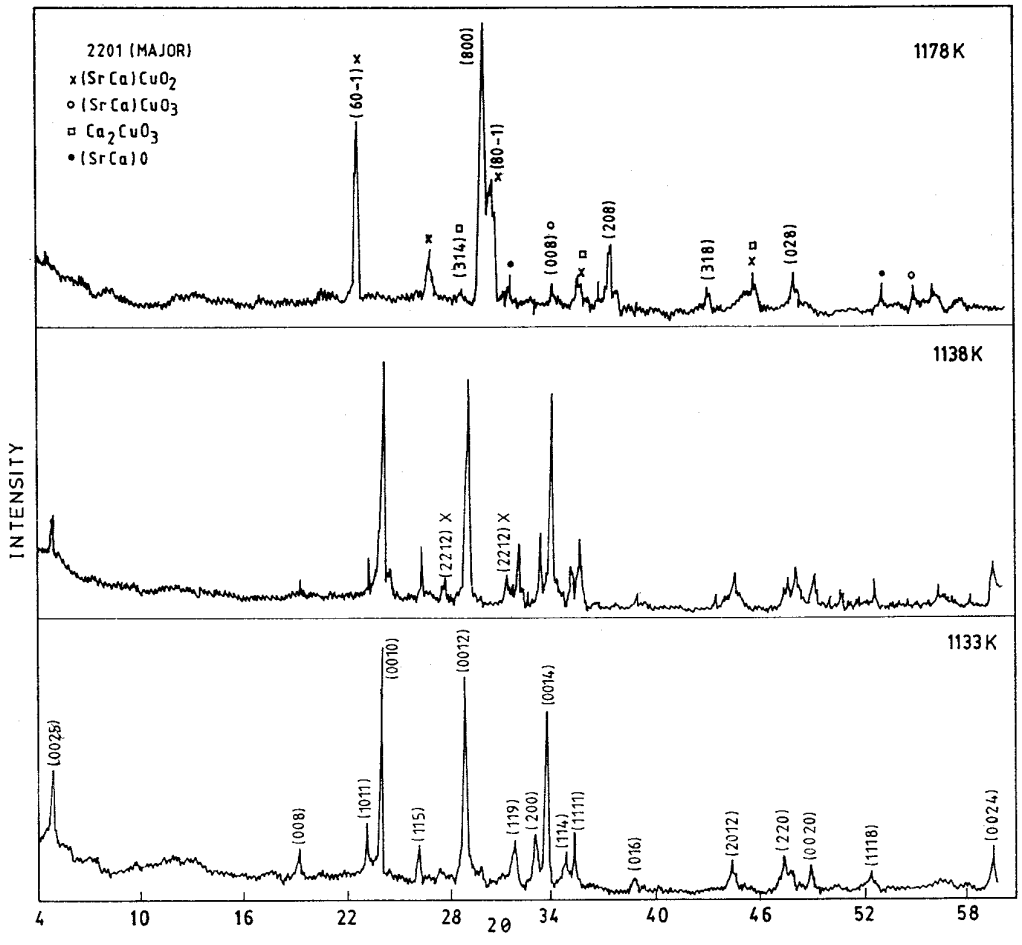

FIG. 9. XRD patterns of samples quenched at various temperatures during the melting of (Bi,Pb)-2223 samples.

$$2212 + 1/2Ca_2CuO_3 + 1/2CuO \xrightarrow{\text{in eutectic melt}} Bi_2Sr_2Ca_2Cu_3O_{10}(2223) \quad [6b]$$

The diffusion of calcium and copper ions in the liquid phase is faster, and the liquid phase (from eutectic) is wettable with the 2212 phase leading to the formation of 2223 phase (29). The absence of an endotherm at 1098 K (Fig. 6) in our samples indicates that the eutectic liquid is not formed in the present system. However, samples heat treated at this eutectic temperature for several weeks do not show the formation of single-phase (Bi,Pb)-2223 compound, the major product is only Bi-2212 phase with traces of 2223 phase. Figure 7 shows the XRD pattern of the sample heat-treated at 1103 K for 600 h, confirming the above results.

3.4. Dissociation of (Bi,Pb)-2223 Phase

DTA studies are conducted in both heating and cooling modes on phase pure samples to study the dissociation of (Bi,Pb)-2223 phase. Figure 8 shows the DTA patterns of pure (Bi,Pb)-2223 compound. During the heating cycle two endotherms are observed at 1076 and 1136 K. Zhang *et al.* have recently attributed the endotherm at 1076 K to the crystalline instability (31). Samples are heat treated to various temperatures corresponding to just below the melting point (1133 K), around the melting point (1138 K), during melting (1148 K), and after melting (1178 K) of (Bi,Pb)-2223 phase and are air quenched from their respective temperatures and characterized by XRD and χ–T measurements. Figure 9 shows the XRD patterns of the quenched samples during melting. The XRD pattern of the sample quenched from 1133 K (Fig. 9a) is identical to that of the starting powder (phase pure (Bi,Pb)-2223 compound). The susceptibility measurements show a sharp diamagnetic signal at 100 K (Fig. 10). The granularity behavior is not observed in this sample compared to sample prepared at 1123 K. The reason for the disappearance of the granularity behavor is not known. The diffractogram of the samples quenched from 1138 and 1148 (Fig. 9b) are

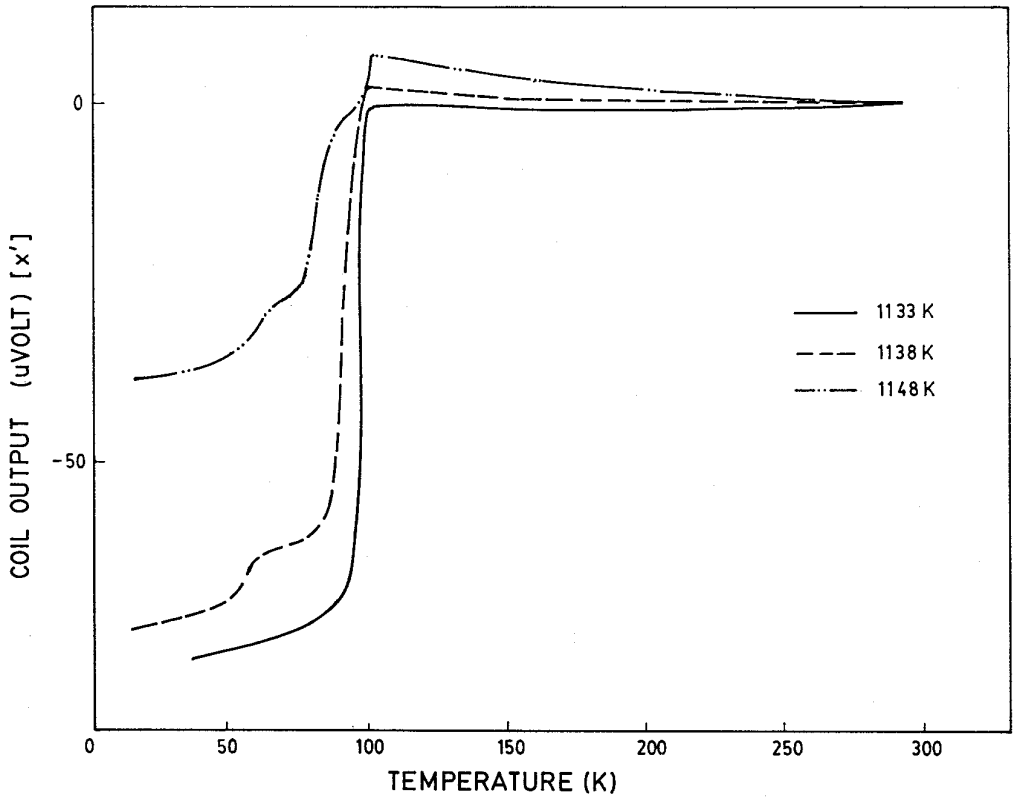

FIG. 10. χ–T plots of (Bi,Pb)-2223 samples quenched from various temperatures.

similar, showing the presence of both (Bi,Pb)-2223 and (Bi,Pb)-2212 phases. Susceptibility measurements (Fig. 10) also show the two-step behavior confirming the presence of both 2212 and (Bi,Pb)-2223 phases. However, the fraction of the (Bi,Pb)-2212 phase is found to be higher in the later sample; i.e., during melting, the (Bi,Pb)-2223 phase decomposes to (Bi,Pb)-2212 phase. The XRD pattern of the sample (Fig. 9c) quenched from 1178 K shows that it contain several phases, namely, Bi-2201, $(Ca,Sr)CuO_3$, $(Ca,Sr)_2CuO_3$, and (Sr,Ca)O, and the sample is found to be nonsuperconducting down to 13 K. Our results match excellently with those of Polonka *et al.* (32). Figure 11 shows the SEM photograph of the sample showing the formation of various precipitates. The probable decomposition reactions of (Bi,Pb)-2223 phase are as follows:

$$\text{(Bi,Pb)-2223} \rightarrow \text{(Bi,Pb)-2212} + Ca_2CuO_3 \qquad [8]$$

simultaneously

$$\text{(Bi,Pb)-2212} \rightarrow \text{Bi-2201} + (Ca,Sr)_2CuO_3 + Ca_2PbO_4 \qquad [9]$$

$$\text{(Bi,Pb)-2212} \rightarrow \text{Bi-2201} + (Ca,Sr)O + Ca_2PbO_4. \qquad [10]$$

The DTA patterns during the cooling cycle are shown in Fig. 8. There are two exotherms with their onset temperatures at 1164 (1153 sh) and 1108 K. The first exotherm at 1164 is highly asymmetric, broad (1164–1108) and is smaller than the melting peak. It is therefore a complicated exotherm representing several processes rather than just simple crystallization. The peaks at 1164 K are due to the

FIG. 11. SEM photograph of decomposed (Bi,Pb)-2223 phase showing formation of various precipitates.

crystallization of 2201 (23) and formation of several phases, as explained above (Fig. 9c). It can be deduced from these studies that the formation and stability regions for (Bi,Pb)-2223 phase are in a very narrow temperature range, 1118 to 1138 K. Any deviation on either side of the temperature leads to the formation of (Bi,Pb)-2212 phase. The other exothermic peak at 1110 K during cooling is due to crystallization of (Bi,Pb)-2212 phase. Since the (Bi,Pb)-2223 phase decomposes to a liquid composition between Bi-2201 and (Bi,Pb)-2212 and calcium cuprates, this thermodynamic information indicates that one route to the formation of (Bi,Pb)-2223 phase is via reaction between the (Bi,Pb)-2212 and Ca_2CuO_3 precursors.

4. CONCLUSIONS

Nearly single-phase (Bi,Pb)-2223 compound has been prepared by the sol–gel process. The mechanism of (Bi,Pb)-2223 phase formation is identified that (Bi,Pb)-2212 phase is reacting with calcium cuprates and copper oxide in the liquid phase obtained by partial melting of calcium-rich 2212 phase. The annealing temperature for the formation of single-phase Bi-2223 compound is found to be 1123 K. The stability region for (Bi,Pb)-2223 compound is found to be 1118 to 1138 K. The dissociation of (Bi,Pb)-2223 phase is established from XRD and DTA studies.

ACKNOWLEDGMENTS

The authors are indebted to Dr. P. Rodriguez, Director, IGCAR, and Professor G. V. Subba Rao, Director, CECRI, Karaikudi, for their constant encouragement during the course of this work. The authors are grateful to Dr. O. M. Sreedharan for useful discussions and suggestions. The authors are thankful to Dr. Sundaram, CECRI, Karaikudi, for allowing the use of the thermal analyzer facility and to Shri. K. Swaminathan of the Metallurgy Division for the DTA facility. Thanks are also due to Dr. M. S. Ramachandar Rao, TIFR, Shri. K. Sankaran, Materials Chemistry Division, and Smt. Radhika, Metallurgy Division, for their help in susceptibility measurements, IR spectra, and SEM pictures, respectively.

REFERENCES

1. C. Michel, M. Hervieu, N. M. Borel, A. Grandin, F. Deslandes, J. Provost, and B. Raveau, *Z. Phys. B* **68,** 421 (1987).
2. H. Maeda, Y. Tanaka, M. Fukotomi, and T. Asano, *Jpn. J. Appl. Phys.* **27,** L209 (1988).
3. P. Majewski, *Adv. Mater.* **6,** 460 (1994).
4. S. A. Sunshine, T. Seigrist, L. F. Schneremeyer, D. W. Murphy, R. J. Cava, B. Batlogg, R. B. van Dover, R. M. Fleming, S. H. Glarum, S. Nakahara, F. Farrow, J. J. Krajewski, S. M. Zahurak, J. V. Waszczak, J. H. Marshall, P. Marsh, L. W. Rupp Jr., and W. F. Peck, *Phys. Rev. B* **38,** 893 (1988).
5. U. Balachandran, S. Shi, D. I. Dos Stantos, S. W. Grahem, M. A. Patel, B. Tami, H. vander Vast, H. Claust, and R. B. Poeppel, *Physica C* **156,** 649 (1989).
6. Y. T. Huang, C. Y. Shei, W. N. Wang, C. K. Chiang, and W. H. Lee, *Physica C* **169,** 76 (1990).
7. M. Huth, M. Scmitt, and H. Adrian, *Physica C* **178,** 203 (1991).
8. T. Hatano, K. Aota, S. Ikeda, K. Nakamura, and K. Ogawa, *Jpn. J. Appl. Phys.* **27,** L2055 (1988).
9. U. Endo, S. Koyama, and T. Kawai, *Jpn. J. Appl. Phys.* **27,** L1467 (1988).
10. H. Sasakura, S. Minamigawa, K. Nakahigachi, M. Kogachi, S. Nakanishi, N. Fukuoka, M. Yoshikawa, S. Noguchi, K. Okuda, and A. Yanasw, *Jpn. J. Appl. Phys.* **28,** L1163 (1989).
11. L. L. Hench and J. K. West, *Chem. Rev.* **90,** 33 (1990).
12. Y. K. Sun and W. Y. Lee, *Physica C* **212,** 37 (1993).
13. H. R. Zhuang, H. Kozuka, and S. Sakka, *J. Mater. Sci.* **25,** 4762 (1990).
14. T. V. Mani, H. K. Varma, K. G. K. Warrier, and A. D. Damodaran, *Br. Ceram. Trans. J* **91,** 120 (1992).
15. S. M. Green, Y. Mei, A. E. Manzi, and H. L. Luo, *J. Appl. Phys.* **66,** 728 (1989).
16. P. Chadda, *in* "Studies of High Temperature Superconductors" (A. V. Narlikar, Ed.), p. 14. Nova Science Publishers, New York.
17. G. B. Deacons and R. J. Phillips, *Coord. Chem. Rev.* **33,** 227 (1980).
18. H. Kozuka, T. Omeda, J. Jin, T. Monde, and S. Sakka, *Bull. Inst. Chem. Res. Kyoto Univ.* **66,** 80 (1988).
19. G. V. Rama Rao, D. S. Suryanarayana, U. V. Varadaraju, G. V. N. Rao, and S. Venkadesan, *J. Alloys Compd.* **217,** 200 (1995).
20. G. V. Rama Rao, D. S. Suryanarayana, U. V. Varadaraju, T. Geethakumari, and S. Venkadesan, *Mater. Chem. Phys.* **39,** 149 (1994).
21. F. G. Alvardo, E. Moran, M. A. A. Franco, M. A. Gonzalez, J. L. Vicant, A. K. Cheetam, and A. N. Chippindales, *J. Less-Common Met.* **164, 165,** 643, (1990).
22. G. R. Paz-Pujalt, *Physica C* **166,** 177 (1990).
23. W. Lo, L. Chen, T. B. Tang, and R. Stevens, *Br. Ceram. Trans. J.* **89,** 218 (1990).
24. G. S. Grader, E. M. Gyorgy, P. K. Gallagar, H. M. O'Bryan, D. W. Johnson Jr., J. Shushine, S. M. Zahurak, S. Jin, and R. C. Sherward, *Phys. Rev. B* **38,** 747 (1988).
25. Y. Yamada, B. Obst, and R. Flukiger, *Super. Cond. Sci. Technol.* **4,** 239 (1991).
26. K. Aota, H. Hattori, T. Hatano, K. Nakamura, and K. Ogawa, *Jpn. J. Appl. Phys.* **28,** L2196 (1989).
27. J. Tsuchiya, H. Endo, N. Kijima, A. Sumiyanama, M. Mizuna, and Y. Oguri, *Jpn. J. Appl. Phys.* **29,** L1918 (1989).
28. S. E. Dorris, B. C. Porodk, M. T. Lanagan, S. Sinha, and R. B. Poeppel, *Physica C* **212,** 60 (1993).
29. Y. Ikeda, H. Ito, S. Shimura, S. Hiroi, M. Takano, Y. Bando, J. Takada, K. Oda, H. Kitaguchi, Y. Mira, Y. Takeda, and T. Takeda, *Physica C* **190,** 18 (1991).
30. Y. L. Chen and R. Stevens, *J. Am. Ceram. Soc.* **75,** 1150 (1992).
31. H. Zhang, F. Ritter, T. Frieling, W. Sun, and W. Assmus, *Solid State Commun.* **92,** 477 (1994).
32. J. Polonka, Ming Xu, Qiang Li, A. I. Goldman, and D. K. Finnemore, *Appl. Phys. Lett.* **59,** 3480 (1991).